Cellular Physiology and Biochemistry

Cell Physiol Biochem 2016;39:205-216
DOI: 10.1159/000445617
Published online: June 24, 2016
Accepted: April 13, 2016

1421-9778/16/0391-0205$39.50/0
www.karger.com/cpb

Original Paper

Microarray Expression Profile of Circular RNAs in Heart Tissue of Mice with Myocardial Infarction-Induced Heart Failure

Hong-Jin Wu[a] Cheng-Ying Zhang[b] Sai Zhang[a] Min Chang[a] Hong-Yun Wang[a]

[a]Beijing Haidian Hospital, Haidian Section of Peking University Third Hospital, Beijing, [b]Traditional Chinese Medical Hospital of Beijing Huairou Beijing, China

Key Words
Myocardial infarction (MI) • Heart failure (HF) • Microarray • Noncoding RNAs • Circular RNAs

Abstract
Background/Aims: Myocardial infarction (MI) is a serious complication of atherosclerosis associated with increasing mortality attributable to heart failure. This study is aimed to assess the global changes in and characteristics of the transcriptome of circular RNAs (circRNAs) in heart tissue during MI induced heart failure (HF). ***Methods:*** Using a post-myocardial infarction (MI) model of HF in mice, we applied microarray assay to examine the transcriptome of circRNAs deregulated in the heart during HF. We confirmed the changes in circRNAs by quantitative PCR. ***Results:*** We revealed and confirmed a number of circRNAs that were deregulated during HF, which suggests a potential role of circRNAs in HF. ***Conclusions:*** The distinct expression patterns of circulatory circRNAs during HF indicate that circRNAs may actively respond to stress and thus serve as biomarkers of HF diagnosis and treatment.

Introduction

Despite advances in clinical and pharmacological interventions, acute myocardial infarction with subsequent left ventricular dysfunction and heart failure (HF) continues to be a major cause of morbidity and mortality worldwide [1, 2]. Approximately 25 % of individuals with HF demonstrate left ventricular outflow tract (LVOT) obstruction [3]. Coronary artery occlusion leads to myocardial infarction (MI), which causes necrosis to an area of the myocardium, pathological remodeling (cardiac hypertrophy, cell death, and fibrosis), and

H.-J. Wu and C.-Y. Zhang contributed equally to this manuscript.

Hong-Jin Wu
Beijing Haidian Hospital, Haidian Section of Peking University Third Hospital, 29th Zhongguancun Setreet, Haidian District, Beijing,China, 100080 (China)
E-Mail whjyuanzhang@163.com

cardiac dysfunction [4, 5]. It has been accepted that HF is caused predominately by genetic variants. HF has a complex genetic basis [6, 7], and a number of biological molecules are potential biomarkers [8, 9] or therapeutic targets [10].To date, around 1400 mutations have been identified as being responsible for HF pathology and more than 60 % of genetic variants occurred in 9 sarcomeric genes, including MYH7, MYL2 and MYBPC3 [11-14]. However, the molecular mechanisms that underlie the pathogenesis of HF remain largely unknown.

In analyses of the human transcriptome, most transcripts have little or no protein-coding capacity but rather are noncoding RNAs [15], which adds novel content to traditional protein-centric molecular biology [16]. MicroRNAs (miRNAs), a class of small noncoding RNAs, are critical in biology and medicine [17-19]. Long non-coding RNAs (lncRNAs) are involved in a variety of biological processes, such as cell-cycle control, differentiation, apoptosis, chromatin remodeling as well as epigenetic regulation [20, 21]. Circular RNAs (circRNAs) are RNA molecules with covalently joined 3'- and 5' -ends formed by back-splice events thus presenting as covalently closed continuous loops. Hence, circRNAs are characterized by scrambled exons, which were already reported more than 20 years ago [22], but mostly misinterpreted as splicing errors. Only in 2012/2013, circRNAs were rediscovered from RNA sequencing (RNA-seq) data and shown to be widespread and diverse in eukaryotic cells [23-25]. CircRNAs in their proposed function as miRNAs sponges are believed to negatively regulate miRNAs, thus contributing substantially to the competing endogenous RNA netword. Therefore, circRNAs are becoming important biological molecules for understanding the mechanisms of disease and for exploring biomarkers for disease diagnosis and treatment.

In order to reveal the potential roles of circRNAs in the pathogenesis of HF, we performed microarray analysis to identify dysregulated circRNAs in heart tissue of mice with myocardial infarction induced heart failure, compared to sham groups. In the present study, we identified a number of circRNAs that are up-regulated or deregulated in heart tissue, and shown that circRNAs play roles in HF, and may represent a novel approach for HF diagnosis and treatment.

Materials and Methods

Materials

Masson's Trichrome Stain Kit was from Abcam (MA, USA); TRIZOL reagent was from Invitrogen (NY, USA). RNeasy minicolumn was from Qiagen (Valencia, CA). The GoScript Reverse Transcription System (cDNA synthesis kit) and Go Taq qPCR Master Mix (SYBR green assay) were from Promega (Madison, WI). Other chemicals and reagents were of analytical grade.

Animal care

Male C57BL/6J mice (18 – 20 g) used in this study were provided by the Animal Department, Health Science Center, Peking University. All animal care and experimental protocols complied with the Animal Management Rules of the Ministry of Health of the People's Republic of China and the guide for the Care and Use of Laboratory Animals published by the US National Institutes of Health (NIH publication No. 85-23, revised 1996). All animals were housed in SPF class condition and were euthanized under sodium pentobarbital anesthesia.

HF model

The acute HF mouse model was induced by permanent ligation of the left anterior descending coronary artery, as previously described [26]. In the operation, electrocardiograms showed ST-elevated MI. mice in the sham-operated group underwent the same surgical procedure, including thread-drawing - but not ligation - at the same site.

Echocardiography

The animals were assessed via a 10S phased array probe (11.5 MHz) and a Vivid 7 Dimension system (GE Healthcare Ultrasound, Horten, Norway). Eight weeks after the surgery, all the mice were anesthetized

with 10% chloral hydrate for the non-invasive examination. The parameters measured were the following: the left ventricular internal dimension at end diastole (LVIDd), interventricular septal thickness at end diastole (IVSd), left ventricular posterior wall thickness at end diastole (LVPWd), left ventricular fractional shortening (FS%) and ejection fraction (EF%). All parameters were measured 5 times by the same observer in a blinded manner, with the final result being the average of the 5.

Histological determination of fibrosis

Fresh heart ventricles from the sham-operated mice (n = 10) and the HF mice (n = 10) were fixed using 4% paraformaldehyde, dehydrated with alcohol, embedded in paraffin and cut into 5-mm-thick slices using a rotary microtome (RM2016; Leica Microsystems, Wetzlar, Germany). The slices were then stained with Masson's trichrome, and observed at x200 magnification using an inverted microscope (IX71; Olympus, Tokyo, Japan).

Western blot analysis

Proteins were prepared as described previously[15]. Freeze-clamped LV tissues (200 - 300 mg) were homogenized briefly in 10 volumes of lysis buffer containing (in mM) 20 Tris-HCl (pH, 7.4), 150 NaCl, 2.5 EDTA, 50 NaF, 0.1 Na4P2O7, 1 Na3VO4, 1 PMSF, 1 DTT, 0.02% (v/v) protease cocktail (Sigma-Aldrich, Missouri, USA), 1% (v/v) Triton X-100 and 10% (v/v) glycerol. The homogenates were centrifuged twice at 20,000 g at 4°C for 15 min, and the supernatants were saved as total proteins. Protein concentrations were determined by the BCA method. Western blot analysis of BNP was performed by loading 20ug of total protein per well on an SDS-PAGE gel. Proteins were transferred to a PVDF membrane (Bio-Rad, California, USA), blocked with 5% non-fat dry milk and probed with specific anti-brain natriuretic protein (BNP) (Ab19645, Abcam, USA) antibody at dilution of 1:1000 and anti-glyceraldehyde-3-phosphate dehydrogenase (GAPDH) (Ab8245, Abcam, USA) at dilution of 1:5000. The immunoreaction was visualized using HRP-conjugated goat anti-rabbit IgG secondary antibody (sc-2357, Santa Cruz Biotechnology, USA) and enhanced chemiluminescent detection kit (Amersham, London, UK), exposed to X-ray film, and quantified by densitometry with a video documentation system (Gel Doc 2000, Bio-Rad, California, USA).

RNA extraction

Ten mice each group were euthanized and hearts were quickly removed and rinsed with cold sterile phosphate buffered saline (PBS; prepared with DEPC water), about 20 mg left ventricular tissues was collected and stored in liquid nitrogen. Five samples of about 100 mg left ventricular tissues were collected, and total RNA was extracted by use of TRIZOL reagent (Invitrogen, NY, USA). Other heart tissues were collected, and total RNA was extracted, then cDNA for quantitative PCR analysis were synthesized from 1 ug of total RNA. Tissues were homogenized in TRIZOL reagent (Invitrogen, USA) using a Qiagen Tissuelyser. Total RNA was extracted in accordance with the manufacturer's protocol and then quantified using a NanoDrop ND-1000 spectrophotometer (Thermo Fisher Scientific, Waltham, MA). RNA integrity of each sample was assessed by denaturing agarose gel electrophoresis.

Labeling and hybridization

Sample labeling and array hybridization were performed according to the manufacturer's protocol (Arraystar, Rockville, Maryland, USA). In short, circRNAs were treated with Ribonuclease R (RNase R) to remove linear RNAs according to the manufacturer's protocol (Epicenter, Madison, WI, USA). Then, each sample was amplified and transcribed into fluorescent cRNA utilizing a random priming method with a Super RNA Labeling Kit (Arraystar). The labeled cRNAs were purified using an RNeasy Mini Kit (Qiagen, Hilden, Germany). The concentration and specific activity of the labeled cRNAs (pmol Cy3/μg cRNA) were measured using NanoDrop ND-1000. Then, 1 μg of each labeled cRNA was fragmented by adding 5 μl 10× Blocking Agent and 1 μl of 25× Fragmentation Buffer. The mixture was heated at 60°C for 30 min, and 25 μl 2× Hybridization buffer was added to dilute the labeled cRNA. Then, 50 μl of the hybridization solution was dispensed into the gasket slide, which was assembled with Mouse Circular RNA Array slides. The slides were incubated for 17 h at 65°C in an Agilent Hybridization Oven. The hybridized arrays were washed, fixed and scanned using an Agilent G2505C Scanner.

Table 1. Specific circRNAs primers for quantitative PCR analysis. PS, product size

Name	Sequence	PS (bp)	Name	Sequence	PS (bp)
GAPDH	F:5'GTTGTCTCCTGCGACTTCA3' R:5'GCCCCTCCTGTTATTATGG3'	293	mmu_circRNA_002690	F: 5' TATCTATGAGCAAGAAACTACT3' R: 5' TGAGTGATCTTAAAGGATAA3'	121
mmu-circRNA_CDR1as	F:5' ACAACTGCGCAGTGTCTCCAG 3'R:5'TTGGAAGACATATATCATCTG 3'	210	mmu_circRNA_002279	F: 5' ATTGTCTCTTGAAGATGAAAT3' R: 5'GTCTCTCAAGTCCCATTA3'	172
mmu_circRNA_001598	F:5'GTGGAGGAGTGGTCGGACAT3' R:5'AAGTAAATGGTCTGCCTGTTGG3'	281	mmu_circRNA_004768	F: 5' TATGACCAGTGTCGTATACAG3' R:5' CTTAGTAGGGGGCTCCTGGCT3'	62
mmu_circRNA_004775	F:5'TTCCTCAAGGCCCAGGCTGCTTTC3' R: 5'CCATGTTCCTGACCTTCTCCAT3'	122	mmu_circRNA_008398	F:5'TGATTAAACTGGGGCTCAGACTT3' R:5' CTGACGTTAGCTGGGACAGGTGG3'	192
mmu_circRNA_005046	F:5'ACCTTGGGAAGAGAAAGAAG3' R:5'CCGGCTCTTCTTTGAGTGA 3'	155	mmu_circRNA_008640	F: 5' TGTGCCTGGAGAGGATCCAGA3' R: 5' GTCAGGGAGAGCTGCAGGGTT3'	168
mmu_circRNA_007687	F:5'AACTTCTCAATACGGCCATCAC3' R:5'TCAAATCTTTCGTTACCATCCC3'	238	mmu_circRNA_010147	F:5'CTATGCTTTCCTGCTGTTCCA3' R:5'CTAGAGTAGCGTTCCACTCGTTC3'	245
mmu_circRNA_013216	F:5'TCGATGAGTACAGGTCTAACCCTA3' R:5'GATAACTCCTCCAGGCTTAGTCTAG3'	46	mmu_circRNA_014961	F:5'TGGACCTGGGCTACAGACTCTT3' R:5'CTCCTGCCAGTCGATCACAAC3'	165
mmu_circRNA_010567	F:5'TAAGCTTCAGGAAATCGAATTGGA3' R:5'GGACAGACATCAACACTGTTCCA 3	177	Helz	F:5'ATACTGCAGCAGCAGGAGAC3' R:5'GGTGGACAGTCTTCACCCAG3'	166
mmu_circRNA_015487	F:5'AGCTTTTCCAGTTCTGGTCA3' R:5'GGAGACTTGGTCCTTCAGC3'	127	Sulf1	F:5'CTGTGCTGAGTGCTTGAGGA3' R:5'GGAGAAGACCACACAGCTCC3'	118
mmu_circRNA_015506	F:5'GGTGGCGGGAAGATGACTGT3' R:5'CCGTCGTAATACTCCACGCTGT3'	175	Zswim6	F:5'TGGCACAGTGACAGAACCTG3' R:5'GCTTCTGTGCAGTTGGCAAG3'	296
mmu_circRNA_016128	F:5' CTTCTGGTTCCTGGAGTTGG3' R:5' AGTTCTGGGATGCTTGCTTTA3'	160	Flnb	F:5' GGGGAAAGTAACCTGCGTGA3' R:5' GACATGCATTTACCGGTGCC3'	277
mmu-circRNA_000174	F: 5' TCAGTGCCTCTCTGCTGAAGA3' R: 5' TTCATTAACTGGGAGTTTGA3'	172	Ubxn1	F:5' CTCGTCCCTGGGTCTCCC3' R:5'TCTCCAGAGGCTCATCCACA3'	210
mmu_circRNA_001135	F: 5' CTTTACCATGTTTGTGACCTC3' R: 5' GAACCAGGATCCAAATGTA3'	138	Zmiz1	F:5' CATCCCTCCACATACTCGGC3' R:5' GGTGGGACCCATCTGGAAAG3'	193
mmu_circRNA_002007	F: 5' AGCTGGCGTGGGGGACATC3' R: 5' GCTGTGTAGATGTCAAAATAG3'	71			

Microarray and quality control

Scanned images were imported into Agilent Feature Extraction software (version 11.0.1.1) for raw data extraction. Quantile normalization of raw data and subsequent data processing were performed using the R software package (R version 3.1.2). After quantile normalization of the raw data, low intensity filtering was performed, and circRNAs with at least 2 out of 8 samples that had flags in "P" or "M" ("All Targets Value") were retained for further analyses. The log2-ratio was used for quantile normalization. CircRNAs differentially expressed between the two groups were conveniently estimated by fold-change filtering and Student's t-test. CircRNAs exhibiting fold changes ≥ 2.0 and p-values ≤ 0.05 were selected as significantly differentially expressed circRNAs. The experiment workflow is listed in Fig. 2.

Quantitative PCR Analysis

cDNA samples were prepared from total RNA of heart tissues by reverse transcription. In total, 10 up-regulated circRNAs and 10 down-regulated circRNAs were analyzed by SYBR green I dye-based detection with specific primer sequences (Table 1). The relative expression of circRNAs was determined by the $2^{(-\Delta\Delta Ct)}$method with housekeeping gene-GAPDH expression to normalize the data.

Statistical analysis

The statistical significance of microarray data was analyzed in terms of fold change using the Student's t-test and FDR was calculated to correct the P-value. FC ≥ 1.5 and P < 0.05 were used to screen the differentially expressed circRNAs. For other statistical analysis, GraphPad Prism 5 software and Microsoft Office software were applied. Stusent's t-test was applied for comparison of two groups and differences with P < 0.05 were considered statistically significant.

Results

Functional evaluation of the mouse HF model

As revealed by echocardiography, HF resulted in a significant decrease contractile function as shown by percent of ejection fraction and fractional shortening (Fig. 1A). We confirmed the permanent ligation of the left anterior descending coronary artery -induced HF in mice as elevated protein level of brain natriuretic protein (BNP, a molecular marker of HF; Fig. 1B). Consistently, significant cardiac and perivascular fibrosis indicated by the staining

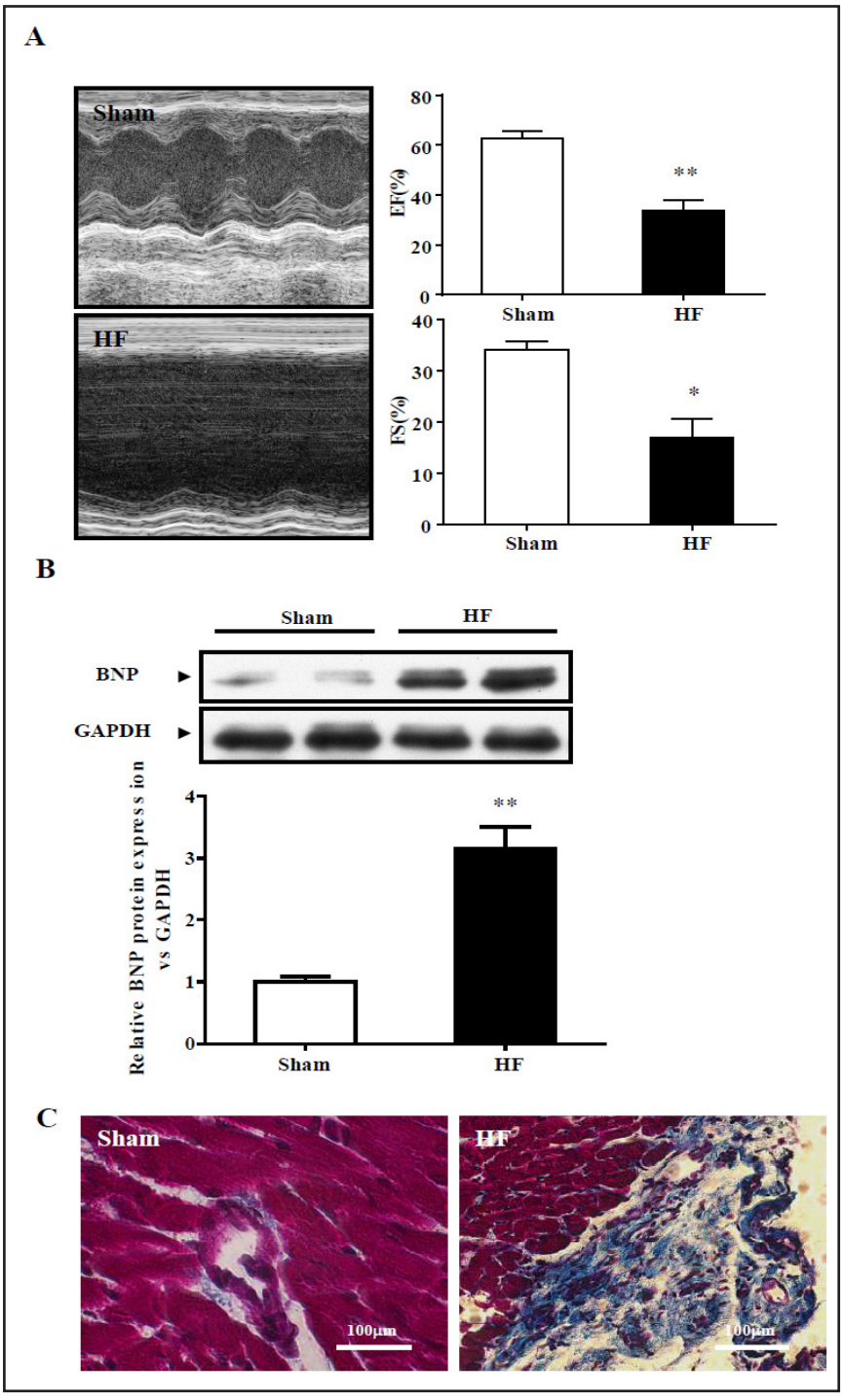

Fig. 1. Functional evaluation of the mouse HF model by echocardiography, BNP pretein, and Masson's trichrome staining. (A) Representative image of echocardiography and the analysis data of percent of ejection fraction (EF%) and fractional shortening (FS%). (B) Representative immunoblots and averaged data for BNP protein expression. (C) Masson's trichrome staining. Values are the mean ± SEM. *p < 0.05, **p<0.01 vs. sham group.

of Masson's trichrome (Fig. 1C) was observed in the HF mice compared with the sham-operated group. All these pathological modifications were linked to ventricular contractile deficiency and caused severe damage to heart function.

Analysis of differentially expressed circRNAs

In total, 1163 circRNAs were detected by Arraystar mouse circRNA Microarray. From the circRNA expression profiles, differentially expressed circRNAs were discriminated between HF and sham group. Hierarchical Clustering was performed to group circRNAs based on their expression levels among samples (Fig. 3A). We set a threshold as log2 fold-change >1.5 (Fig.

3B) and P-value < 0.05 (Fig. 3C), and found that a total of 63 circRNAs were differentially expressed, consisting of 29 up-regulated circRNAs (Table 2) and 34 down-regulated circRNAs (Table 3). We summarized the classification of dysregulated circRNAs. Among the up-regulated circRNAs, there were 5 intergenic, 1 antisense, 1 intragnic and 22 exonic (Fig. 3D). Among the down-regulated circRNAs, there were 5 intergenic, 2 antisense, 1 intragenic and 26 exonic (Fig. 3D).

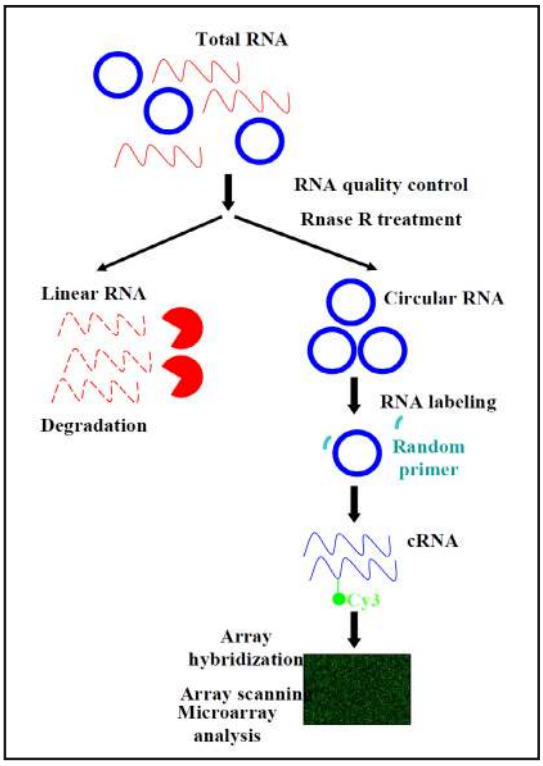

Fig. 2. Experiment workflow of microarray expression profile of circular RNAs.

Real-time PCR validation of some differentially expressed circRNAs

We randomly selected 20 dysregulated circRNAs including 10 up-regulated circRNAs (CDR1as, 001598, 004775, 005046, 007687, 013216, 010567, 015487, 015506 016128) and 10 down-regulated circRNAs (000174, 001135, 002007, 002690, 002279, 004768, 008398, 008640, 010147 and 014961) for verification in these myocardial tissues samples. A general consistency was shown between the real-time PCR and microarray analysis results. Six selected circRNAs in terms of up-regulated circRNAs (Fig. 4A) and six selected circRNAs in terms of down-regulated circRNAs(Fig. 4B) were confirmed. Interestingly, circRNAs expression did not correlate with the expression of the host genes suggesting an independent regulation of transcription versus circRNA formation (Fig. 4C).

Prediction of the circRNA/microRNA interaction

Recent evidences have demonstrated that circular RNAs play a crucial role in fine tuning the level of miRNA mediated regulation of gene expression by sequestering the miRNAs. Their interaction with disease associated miRNAs indicates that circular RNAs are important for disease regulation [27-29]. To find the potential miRNA target, two confirmed circRNAs (mmu_circRNA_013216 and mmu_circRNA_010567) were selected and the circRNA/microRNA interaction was predicted with Arraystar's home-made miRNA target prediction software based on TargetScan& miRanda. The potential miRNA targets of mmu_circRNA_013216 include miR-181a-3p, miR-486a-5p and miR-486b-5p (Fig. 5A). For mmu_circRNA_010567, the potential miRNA targets include miR-124. miR-141 and miR-200a (Fig. 5B). It has been shown that miRNA-141 could regulate the expression level of ICAM-1 on endothelium to decrease myocardial ischemia-reperfusion injury [30], while the function of the most potential miRNAs on heart are far from clear.

Discussion

In the present study, we performed a comprehensive analysis of dysregulated circRNAs by comparing the transcriptome profiles of hypertrophied myocardial tissues with or without heart failure. A total of 1163 circRNAs were detected. We identified 29 up-regulated and 34 down-regulated circRNAs, and summarized their general characteristics. Thus, our study could provide a comprehensive understanding of circRNAs in heart failure heart and help to elucidate the molecular mechanisms of Heart failure.

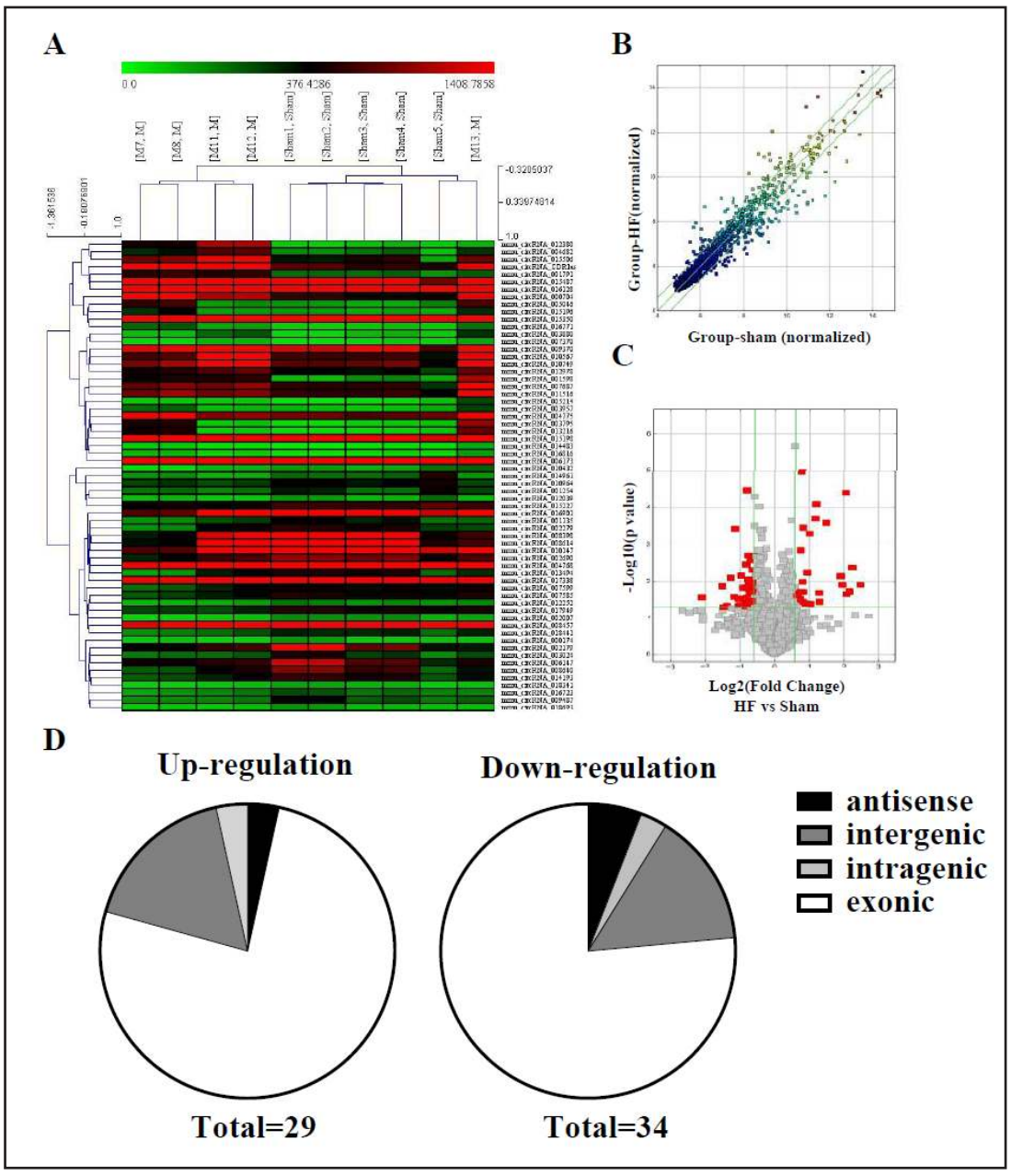

Fig. 3. Analysis of differentially expressed circRNAs. (A) The hierarchical clustering of partial differentially expressed circRNAs. 'Red' indicates high relative expression, and 'green' indicates low relative expression. (B) CircRNAs in the Scatter-Plot above the top green line and below the bottom green line indicated more than 1.5 fold change of circRNAs between the two compared samples. (C) CircRNAs (red point) in the Volcano Plots represents the 1.5-fold up and down expressed circRNAs with statistical significance ($P < 0.05$). (D) classification of dysregulated circRNAs.

Large amounts of circRNAs are recently discovered and represent a new special class of endogenous noncoding RNA. Recent researches have revealed that circRNAs are an abundant, stable, diverse and conserved class of RNA molecules [20-22]. Moreover, circRNAs can function as miRNA sponges or regulate parent gene expression to affect disease initiation and progression [27, 28, 31]. A recent report shows that circRNA ciRS-7 acts as a miR-7 sponge to suppress miR-7 activity, resulting in increased levels of miR-7 targets [29]. Other

Table 2. Up-regulated circRNAs between HF heart tissues and sham tissues. FC, fold change, FDR, false discover rate

circRNA	P-value	FDR	FC	Regulation	circRNA_type	chrom	strand	best_transcript	Gene Symbol
mmu_circRNA_CDR1as	0.000	0.030	2.816	up	antisense	chrX	+	NM_001166658	Cdr1
mmu_circRNA_000704	0.012	0.188	3.900	up	exonic	chr7	+	NM_011858	Tenm4
mmu_circRNA_001598	0.000	0.012	4.196	up	exonic	chr9	+	NM_001025600	Cadm1
mmu_circRNA_001791	0.043	0.301	2.057	up	exonic	chr13	-	NM_019930	Ranbp9
mmu_circRNA_003795	0.020	0.222	4.484	up	intragenic	chr1	-	NM_001039184	Cep350
mmu_circRNA_003880	0.040	0.291	2.066	up	exonic	chr11	+	NM_001159404	Llgl1
mmu_circRNA_003957	0.021	0.226	1.613	up	exonic	chr12	+	NM_172803	Dock4
mmu_circRNA_004682	0.035	0.276	2.470	up	exonic	chr18	-	NM_134134	Hmgxb3
mmu_circRNA_004775	0.039	0.289	1.866	up	exonic	chr2	-	NM_146122	Dennd1a
mmu_circRNA_005046	0.021	0.226	2.460	up	exonic	chr5	-	NM_177047	Auts2
mmu_circRNA_005214	0.035	0.276	1.764	up	intragenic	chr10	-	NR_028262	Rmst
mmu_circRNA_007370	0.030	0.257	1.567	up	exonic	chr9	-	NM_001042752	Neo1
mmu_circRNA_007687	0.001	0.035	2.033	up	exonic	chr11	+	NM_198298	Helz
mmu_circRNA_009370	0.019	0.222	1.772	up	intragenic	chr17	+	uc012ath.2	Rn45s
mmu_circRNA_010567	0.010	0.171	1.752	up	exonic	chr13	-	NM_145456	Zswim6
mmu_circRNA_010749	0.006	0.134	1.936	up	intragenic	chr17	+	uc012ath.2	Rn45s
mmu_circRNA_011516	0.000	0.006	1.718	up	intronic	chr15	-	NM_001013360	Npcd
mmu_circRNA_012380	0.012	0.188	5.577	up	exonic	chr16	-	NM_007938	Epha6
mmu_circRNA_012978	0.001	0.080	1.692	up	intronic	chr17	-	uc008awy.1	Tsc2
mmu_circRNA_013216	0.022	0.226	4.219	up	intragenic	chr1	+	NM_001198565	Sulf1
mmu_circRNA_014483	0.030	0.257	1.671	up	exonic	chr15	+	NM_011767	Zfr
mmu_circRNA_015196	0.024	0.239	1.570	up	exonic	chr13	-	NM_001122989	Cdc14b
mmu_circRNA_015198	0.019	0.222	1.684	up	exonic	chr5	+	NM_175473	Fras1
mmu_circRNA_015350	0.000	0.028	2.275	up	exonic	chr1	-	NM_001077695	Ncoa2
mmu_circRNA_015487	0.004	0.120	4.748	up	exonic	chr7	+	NM_011565	Tead2
mmu_circRNA_015506	0.007	0.142	3.770	up	exonic	chr17	+	NM_015800	Crim1
mmu_circRNA_016128	0.018	0.221	4.466	up	exonic	chr7	+	NM_153591	Nars2
mmu_circRNA_016771	0.000	0.016	2.314	up	exonic	chr2	-	NM_001141931	Rbms1
mmu_circRNA_016816	0.000	0.032	1.770	up	exonic	chr14	+	uc007suc.1	Erc2

Table 3. Down-regulated circRNAs between HF heart tissues and sham tissues. FC, fold change, FDR, false discover rate

circRNA	P-value	FDR	FC	Regulation	circRNA_type	chrom	strand	best_transcript	Gene Symbol
mmu_circRNA_000174	0.024	0.239	1.641	down	exonic	chr1	-	NM_027671	Sntg1
mmu_circRNA_001135	0.030	0.257	1.771	down	exonic	chr14	+	NM_026283	Samd8
mmu_circRNA_001254	0.022	0.226	1.632	down	exonic	chr5	-	uc008xwx.1	Epha5
mmu_circRNA_002007	0.000	0.032	2.197	down	intragenic	chr14	+	NM_134080	Flnb
mmu_circRNA_002179	0.026	0.247	2.246	down	exonic	chr6	-	NM_001136065	Hipk2
mmu_circRNA_002279	0.029	0.257	2.045	down	exonic	chrX	+	NM_001034907	Zc3h12b
mmu_circRNA_002690	0.028	0.257	1.731	down	exonic	chr2	-	NM_172664	Tlk1
mmu_circRNA_003024	0.036	0.276	1.652	down	exonic	chr18	-	NM_001201569	Atp9b
mmu_circRNA_004768	0.015	0.198	1.884	down	intragenic	chr19	+	NM_146093	Ubxn1
mmu_circRNA_006147	0.043	0.301	1.734	down	exonic	chr5	-	NM_194340	Prr14l
mmu_circRNA_006173	0.002	0.090	1.679	down	intragenic	chr12	-	NM_001146176	Max
mmu_circRNA_007585	0.005	0.124	1.550	down	exonic	chr2	+	NM_001080754	Ambra1
mmu_circRNA_007599	0.019	0.222	1.533	down	intragenic	chr1	-	NM_008551	Mapkapk2
mmu_circRNA_008398	0.045	0.303	2.587	down	exonic	chr9	-	ENSMUST00000183955	Mlip
mmu_circRNA_008457	0.002	0.090	1.500	down	exonic	chr16	-	NM_001145886	Tiam1
mmu_circRNA_008614	0.050	0.319	2.763	down	exonic	chr9	-	ENSMUST00000183955	Mlip
mmu_circRNA_008640	0.046	0.303	2.048	down	exonic	chr6	+	ENSMUST00000070736	Adcyap1r1
mmu_circRNA_009487	0.003	0.115	1.752	down	exonic	chr6	-	NM_001159533	Cacna1c
mmu_circRNA_010147	0.027	0.250	4.273	down	exonic	chr19	-	NM_198300	Cpeb3
mmu_circRNA_010432	0.047	0.306	1.875	down	exonic	chr4	-	NM_001081557	Camta1
mmu_circRNA_010964	0.011	0.181	1.659	down	intergenic	chr1	+		
mmu_circRNA_012039	0.007	0.142	1.942	down	exonic	chr2	+	NM_001039939	Asxl1
mmu_circRNA_012252	0.003	0.096	1.610	down	exonic	chr16	-	NM_175549	Robo2
mmu_circRNA_013494	0.044	0.303	1.984	down	intronic	chr9	+	NM_011029	Rpsa
mmu_circRNA_014193	0.016	0.203	1.670	down	exonic	chr2	-	uc008nmu.1	Rbm39
mmu_circRNA_014961	0.008	0.147	2.401	down	exonic	chr14	+	NM_183208	Zmiz1
mmu_circRNA_015227	0.009	0.158	1.684	down	exonic	chr5	+	NM_001243123	Fam193a
mmu_circRNA_016723	0.014	0.193	1.579	down	antisense	chr2	-	NM_011701	Vim
mmu_circRNA_016901	0.014	0.193	1.703	down	exonic	chr17	+	NM_134117	Pkdcc
mmu_circRNA_017338	0.014	0.193	2.854	down	exonic	chr10	+	NM_001111065	Reps1
mmu_circRNA_017949	0.000	0.012	1.728	down	exonic	chr6	-	NM_001081206	Dgki
mmu_circRNA_018341	0.034	0.274	1.568	down	exonic	chrX	-	ENSMUST00000101616	Smarca1
mmu_circRNA_018441	0.010	0.171	1.546	down	antisense	chr1	+	NM_201364	BC055324
mmu_circRNA_018693	0.019	0.222	1.550	down	exonic	chr5	+	NM_198702	Lphn3

study also shows that a human circRNA CDR1as functions to bind miR-7 in neuronal tissues and sequesters away the miR-7 from its target sites [25]. In this study, we found a lot

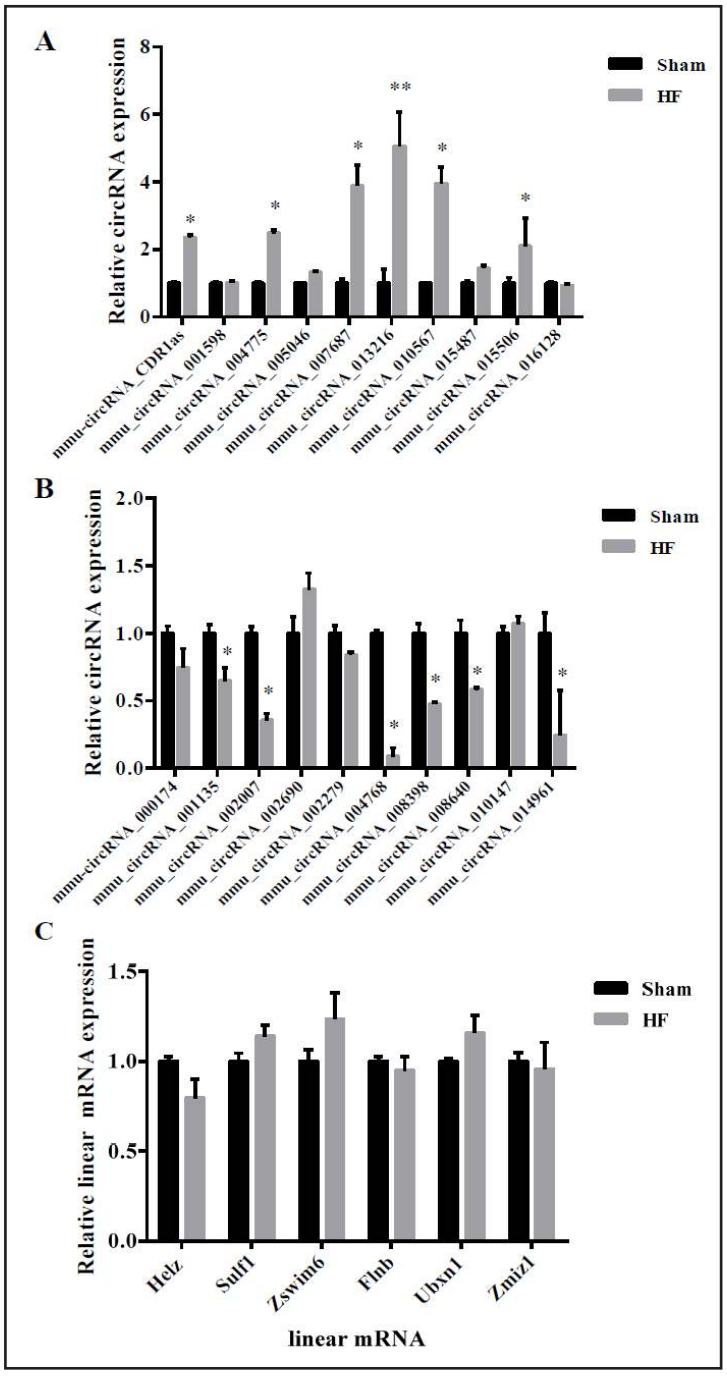

Fig. 4. Real-time PCR validation of some differentially expressed circRNAs and mRNA from microarray data. Twenty circRNAs were chosen for real-time PCR validation. Fold changes were calculated by the $2^{\wedge(-\Delta\Delta Ct)}$ method. Data shown are representative of 5 HF tissues and 5 controls; Values are the mean ±SEM. *p < 0.05, **p < 0.01 vs. sham group.

of dysregulated circRNAs in heart tissue during MI induced heart failure (HF) and predicted the circRNA/microRNA interaction with Arraystar's home-made miRNA target prediction software based on TargetScan & miRanda. For example, among the founded potential circRNA/microRNA interactions, up-regulated circRNA mmu_circRNA_010567 is potential to be a sponge of miR-141. Moreover, miRNA-141 regulates the expression level of ICAM-1 on endothelium to decrease myocardial ischemia-reperfusion injury [30]. Meanwhile, mmu_circRNA_010567 may represent a new type of mediator of heart failure occurrence and development. However, due to the limited known function of circRNAs and miRNAs, a lot of circRNA/microRNA interactions should be analyzed in the future. More importantly, by further studying the functions of circRNAs, we could improve our understanding of the

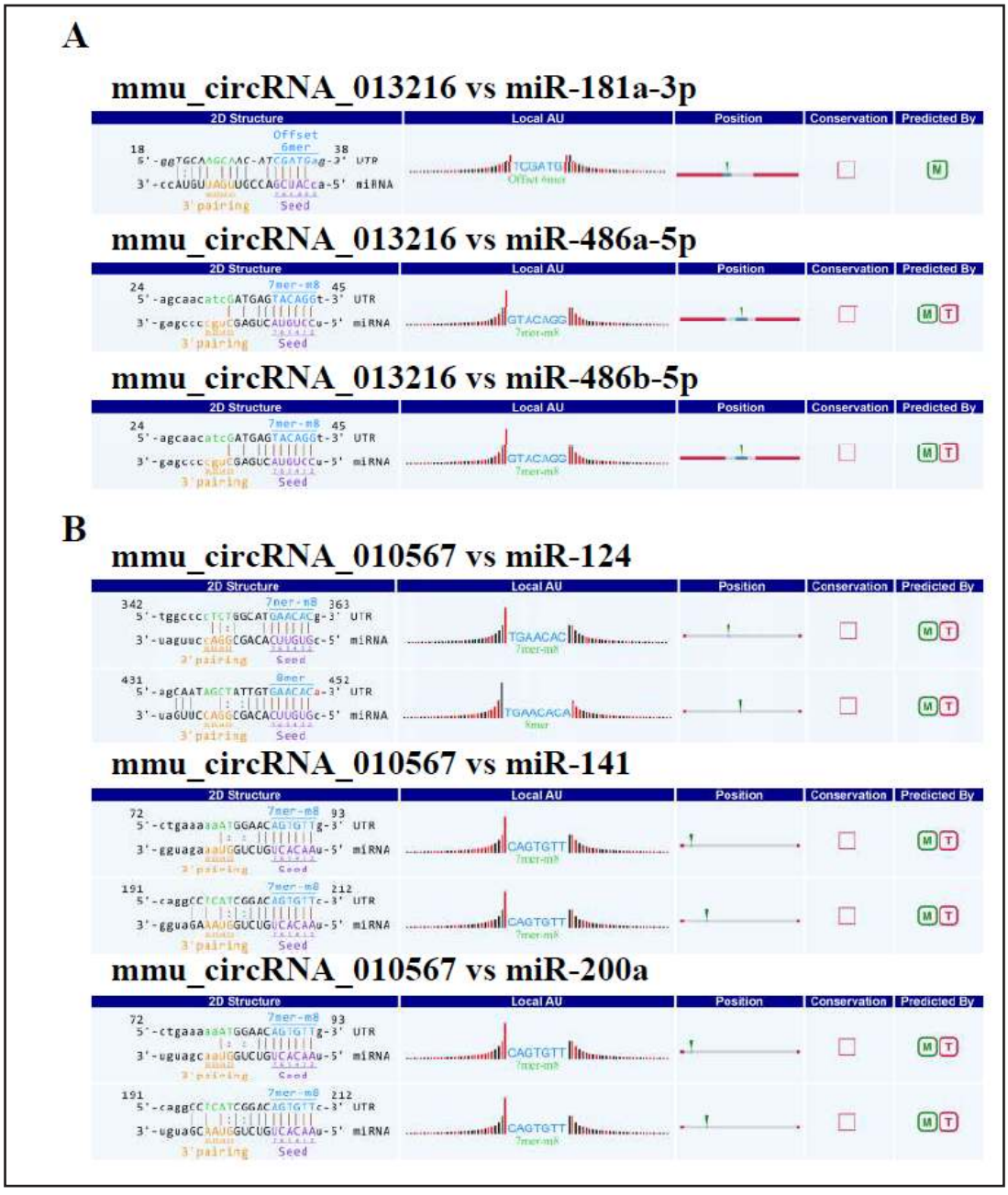

Fig. 5. A snippet of the detailed annotation for circRNA/miRNA interaction ((A) mmu_circRNA_013216; (B) mmu_circRNA_010567).

mechanisms of disease associated with circRNAs and improve the diagnosis and prevention of circRNA-associated diseases.

Acknowledgments

This project was supported by Grants from the National Natural Science Foundation of China (nos. 81273890 and 81173367).

Disclosure Statement

The authors declare that there are no conflicts of interest.

References

1 Gerczuk PZ, Kloner RA: An update on cardioprotection: a review of the latest adjunctive therapies to limit myocardial infarction size in clinical trials. J Am Coll Cardiol 2012;59:969-978.
2 Roger VL, Go AS, Lloyd-Jones DM, Benjamin EJ, Berry JD, Borden WB, Bravata DM, Dai S, Ford ES, Fox CS, Fullerton HJ, Gillespie C, Hailpern SM, Heit JA, Howard VJ, Kissela BM, Kittner SJ, Lackland DT, Lichtman JH, Lisabeth LD, Makuc DM, Marcus GM, Marelli A, Matchar DB, Moy CS, Mozaffarian D, Mussolino ME, Nichol G, Paynter NP, Soliman EZ, Sorlie PD, Sotoodehnia N, Turan TN, Virani SS, Wong ND, Woo D, Turner MB, American Heart Association Statistics C, Stroke Statistics S: Heart disease and stroke statistics--2012 update: a report from the American Heart Association. Circulation 2012;125:e2-e220.
3 Vefali H, Manda Y, Shirani J: Myocardial viability in coronary artery chronic total occlusion. Curr Cardiol Rep 2015;17:552.
4 Hou J, Kang YJ: Regression of pathological cardiac hypertrophy: signaling pathways and therapeutic targets. Pharmacol Ther 2012;135:337-354.
5 Ladage D, Tilemann L, Ishikawa K, Correll RN, Kawase Y, Houser SR, Molkentin JD, Hajjar RJ: Inhibition of PKCalpha/beta with ruboxistaurin antagonizes heart failure in pigs after myocardial infarction injury. Circ Res 2011;109:1396-1400.
6 Creemers EE, Wilde AA, Pinto YM: Heart failure: advances through genomics. Nat Rev Genet 2011;12:357-362.
7 Dorn GW, 2nd: The genomic architecture of sporadic heart failure. Circ Res 2011;108:1270-1283.
8 Maisel AS, Choudhary R: Biomarkers in acute heart failure--state of the art. Nat Rev Cardiol 2012;9:478-490.
9 Wang J, Li L, Su Q, Zhou Y, Chen H, Ma G, Liu T, Tang Z, Liu Y: The involvement of phosphatase and tensin homolog deleted on chromosome ten (PTEN) in the regulation of inflammation following coronary microembolization. Cell Physiol Biochem 2014;33:1963-1974.
10 Tamargo J, Lopez-Sendon J: Novel therapeutic targets for the treatment of heart failure. Nat Rev Drug Discov 2011;10:536-555.
11 Roma-Rodrigues C, Fernandes AR: Genetics of hypertrophic cardiomyopathy: advances and pitfalls in molecular diagnosis and therapy. Appl Clin Genet 2014;7:195-208.
12 Efthimiadis GK, Pagourelias ED, Gossios T, Zegkos T: Hypertrophic cardiomyopathy in 2013: Current speculations and future perspectives. World J Cardiol 2014;6:26-37.
13 Nishimura RA, Ommen SR: Hypertrophic cardiomyopathy: the search for obstruction. Circulation 2006;114:2200-2202.
14 Maron BJ, Maron MS, Semsarian C: Genetics of hypertrophic cardiomyopathy after 20 years: clinical perspectives. J Am Coll Cardiol 2012;60:705-715.
15 Bertone P, Stolc V, Royce TE, Rozowsky JS, Urban AE, Zhu X, Rinn JL, Tongprasit W, Samanta M, Weissman S, Gerstein M, Snyder M: Global identification of human transcribed sequences with genome tiling arrays. Science 2004;306:2242-2246.
16 Schonrock N, Harvey RP, Mattick JS: Long noncoding RNAs in cardiac development and pathophysiology. Circ Res 2012;111:1349-1362.
17 Salmena L, Poliseno L, Tay Y, Kats L, Pandolfi PP: A ceRNA hypothesis: the Rosetta Stone of a hidden RNA language? Cell 2011;146:353-358.
18 Wang Y, Men M, Yang W, Zheng H, Xue S: MiR-31 Downregulation Protects Against Cardiac Ischemia/Reperfusion Injury by Targeting Protein Kinase C Epsilon (PKCepsilon) Directly. Cell Physiol Biochem 2015;36:179-190.
19 Zhao X, Wang K, Liao Y, Zeng Q, Li Y, Hu F, Liu Y, Meng K, Qian C, Zhang Q, Guan H, Feng K, Zhou Y, Du Y, Chen Z: MicroRNA-101a inhibits cardiac fibrosis induced by hypoxia via targeting TGFbetaRI on cardiac fibroblasts. Cell Physiol Biochem 2015;35:213-226.

20 Mattick JS: The genetic signatures of noncoding RNAs. PLoS Genet 2009;5:e1000459.
21 Rinn JL, Chang HY: Genome regulation by long noncoding RNAs. Annu Rev Biochem 2012;81:145-166.
22 Nigro JM, Cho KR, Fearon ER, Kern SE, Ruppert JM, Oliner JD, Kinzler KW, Vogelstein B: Scrambled exons. Cell 1991;64:607-613.
23 Salzman J, Gawad C, Wang PL, Lacayo N, Brown PO: Circular RNAs are the predominant transcript isoform from hundreds of human genes in diverse cell types. PLoS One 2012;7:e30733.
24 Jeck WR, Sorrentino JA, Wang K, Slevin MK, Burd CE, Liu J, Marzluff WF, Sharpless NE: Circular RNAs are abundant, conserved, and associated with ALU repeats. RNA 2013;19:141-157.
25 Memczak S, Jens M, Elefsinioti A, Torti F, Krueger J, Rybak A, Maier L, Mackowiak SD, Gregersen LH, Munschauer M, Loewer A, Ziebold U, Landthaler M, Kocks C, le Noble F, Rajewsky N: Circular RNAs are a large class of animal RNAs with regulatory potency. Nature 2013;495:333-338.
26 Zhuang Y, Chen X, Xu M, Zhang LY, Xiang F: Chemokine stromal cell-derived factor 1/CXCL12 increases homing of mesenchymal stem cells to injured myocardium and neovascularization following myocardial infarction. Chin Med J (Engl) 2009;122:183-187.
27 Hansen TB, Kjems J, Damgaard CK: Circular RNA and miR-7 in cancer. Cancer Res 2013;73:5609-5612.
28 Qu S, Yang X, Li X, Wang J, Gao Y, Shang R, Sun W, Dou K, Li H: Circular RNA: A new star of noncoding RNAs. Cancer Lett 2015;365:141-148.
29 Hansen TB, Jensen TI, Clausen BH, Bramsen JB, Finsen B, Damgaard CK, Kjems J: Natural RNA circles function as efficient microRNA sponges. Nature 2013;495:384-388.
30 Liu RR, Li J, Gong JY, Kuang F, Liu JY, Zhang YS, Ma QL, Song CJ, Truax AD, Gao F, Yang K, Jin BQ, Chen LH: MicroRNA-141 regulates the expression level of ICAM-1 on endothelium to decrease myocardial ischemia-reperfusion injury. Am J Physiol Heart Circ Physiol 2015;309:H1303-1313.
31 Li Z, Huang C, Bao C, Chen L, Lin M, Wang X, Zhong G, Yu B, Hu W, Dai L, Zhu P, Chang Z, Wu Q, Zhao Y, Jia Y, Xu P, Liu H, Shan G: Exon-intron circular RNAs regulate transcription in the nucleus. Nat Struct Mol Biol 2015;22:256-264.